Dimensionality of excitons in laser-diode structures composed of $In_xGa_{1-x}N$ multiple quantum wells

Yukio Narukawa, Yoichi Kawakami, and Shigeo Fujita
Department of Electronic Science and Engineering, Kyoto University, Kyoto 606-8501, Japan

Shuji Nakamura
Department of Research and Development, Nichia Chemical Industries Ltd., 491 Oka, Kaminaka, Anan, Tokushima 774-8601, Japan

(Received 9 June 1998; revised manuscript received 6 October 1998)

Temperature dependence of radiative and nonradiative lifetimes of localized excitons has been assessed in the laser diode structures composed of $In_{0.20}Ga_{0.80}N$ (3 nm)/$In_{0.05}Ga_{0.95}N$ (6 nm) multiple quantum well (MQW) [sample (a)] and $In_{0.10}Ga_{0.90}N$ (3 nm)/$In_{0.02}Ga_{0.98}N$ (6 nm) MQW [sample (b)] by means of time-resolved photoluminescence spectroscopy. The radiative lifetimes (τ_{rad}) in sample (a) were almost constant around 6 ns between 23 K and 200 K, suggesting the mesoscopic effect where excitons are confined in the zero-dimensional potential such as a quantum-dot-like region. This interpretation fairly agrees with the result that the emission was ascribed to the localized excitons whose depth is about 250 meV. The τ_{rad} value in sample (b) was 460 ps at 20 K and grew with increasing temperature. It was found that the depth of exciton localization in sample (b) is so weak that excitons reveal a nearly two-dimensional feature at RT as a result of the delocalization effect. [S0163-1829(99)08815-3]

I. INTRODUCTION

GaN-based semiconductors are attracting much interest because the shortest laser diode (LD) operation has been demonstrated under a continuous-wave (CW) mode at room temperature (RT),[1–3] in spite of high dislocation densities in these epilayers grown on sapphire substrates. Although the maximum operation time estimated is reported to be 10 000 h,[4] it is necessary to reduce the lasing threshold-current density to achieve stable operation. Moreover, it should be noted that the tuning wavelength for the stable CW operation of LD's is currently in the range between 380–430 nm, which is much narrower than that of LED's. The reason why the operation wavelength is limited to about 430 nm at the long-wavelength side may be because the optical gain cannot be generated sufficiently in the devices with In-rich active layers due to the inhomogeneous broadening effect, as well as due to the limited number of density of states (DOS). Further breakthrough is therefore required to realize pure blue and green LD's using $In_xGa_{1-x}N$-based semiconductors. Such targets can be facilitated by the well understanding of emission mechanism, as well as by the well designing of the LD structures.

Recently, it has been reported that localized excitons play an important role for the emission mechanism in $In_xGa_{1-x}N$-based multiple quantum wells (MQW's).[5–7] The detailed nature of exciton localization in the $In_{0.20}Ga_{0.80}N/In_{0.05}Ga_{0.95}N$ MQW LD structures was revealed by means of transmittance (TR), electroreflectance (ER), photoluminescence excitation (PLE), and time-resolved PL (TRPL) spectroscopy at 20 K, where the main spontaneous emission was attributed to localized excitons whose trap center is located below the lowest $n=1$ quantized level by about 250 meV.[6] The depth of the trap center was so large that the localized excitons dominated the PL spectra even at RT. Cross-sectional transmission electron microscopy (TEM) and energy-dispersive x-ray microanalysis (EDX) observations revealed that deep localization of excitons (or carriers) originates from the In-rich regions acting as quantum dots (QD's).[8,9] Cathodoluminescence (CL) spectra mapping of $In_{0.20}Ga_{0.80}N$ single quantum wells (SQW's) also revealed that the localization centers are spatially distributed with size less than 60 nm (Ref. 10) whose resolution is limited by the diffusion length of the carriers (or excitons). If such centers are generated by the microstructural disorder as a result of the compositional modulation, the degree of exciton localization may differ depending on the mean In composition in the $In_xGa_{1-x}N$ active layers. Our objective is to elucidate further the microscopic structures and macroscopic optical properties. However, little has been known about the size of localization centers in the plane of quantum wells (i.e., dimensionality), which is an important factor for naming the system quantum disk, mesoscopic dots, or quantum dots. Temperature dependence of radiative lifetimes is one of the most effective macroscopic optical characterizations for the evaluation of dimensionality.[11,12]

Consequently, the assessment is motivated on the dynamical behavior of localized excitons in $In_xGa_{1-x}N$ QW's. In this paper, temperature dependence of radiative and nonradiative lifetimes of localized excitons has been studied in the $In_{0.20}Ga_{0.80}N/In_{0.05}Ga_{0.95}N$ MQW [sample (a)] and the $In_{0.10}Ga_{0.90}N/In_{0.02}Ga_{0.98}N$ MQW [sample (b)] structure by employing TRPL spectroscopy.

II. EXPERIMENTAL PROCEDURE

The samples used in this study were grown on (0001)-oriented sapphire (Al_2O_3) substrates by a two-flow metal-organic chemical vapor deposition (TF-MOCVD)

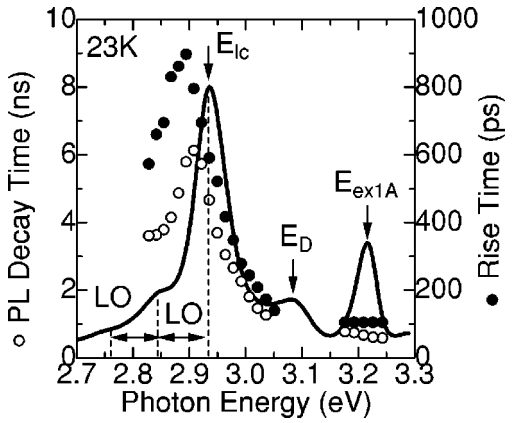

FIG. 1. Time-integrated PL spectrum as well as decay times and rise times of PL as a function of monitored emission energy taken at 23 K under excitation energy density of 120 nJ/cm^2 in sample (a) ($In_{0.20}Ga_{0.80}N/In_{0.05}Ga_{0.95}N$ MQW).

technique.[13] Two types of LD structures, whose In composition in the active layers were roughly (a) 20% and (b) 10%, were assessed in this study. Both samples consist of the separate confinement heterostructure where (a) the undoped $In_{0.20}Ga_{0.80}N$ (3 nm)/$In_{0.05}Ga_{0.95}N$ (6 nm) MQW with seven periods, (b) the Si-doped $In_{0.10}Ga_{0.90}N$ (3 nm)/$In_{0.02}Ga_{0.98}N$ (6 nm) MQW with three periods are sandwiched between GaN waveguide layers (0.1 μm in each) and (a) $Al_{0.15}Ga_{0.85}N$, (b) $Al_{0.07}Ga_{0.93}N$ cladding layers (0.4 μm in each). The top of the $Al_xGa_{1-x}N$ clad and the GaN waveguide are Mg-doped *p*-type layers, while the bottom of the clad and the waveguide are Si-doped *n*-type layers. The LD has been operated at 420 nm under pulsed mode at RT for sample (a), and at 390 nm under CW mode at RT for sample (b).

The TRPL measurements were performed with a fast scan streak camera in conjunction with a 25-cm monochromator using a 100-lines/mm grating for sample (a) and a 300-lines/mm grating for sample (b). Pulsed excitation was provided by the frequency doubled beam of a mode-locked Al_2O_3:Ti laser, which was pumped by an Ar^+ laser. In order to avoid multiexcitation, the repetition rate of the source (80.0 MHz) was selected to 4.0 MHz by the acoustic optic (AO) modulator. The wavelength and the pulse width were 367 nm and 1.5 ps, respectively, by which selective excitation to the $In_xGa_{1-x}N$ QW's can be achieved. The excitation power density (I_{ex}) was kept constant at 120 nJ/cm^2 for sample (a) and 500 nJ/cm^2 for sample (b). The light source used for reflectance, ER, photoinduced voltage (PV), PLE, and low excitation PL was obtained by passing the Xe lamp through a 25-cm monochromator. The ER signal was detected by a Si photodiode and amplified by a lock-in amplifier. The spectral resolution of all measurements was less than 0.3 nm, which is well below the linewidth of the PL.

III. RESULTS AND DISCUSSION

The time-integrated PL spectrum taken at 23 K in the sample (a) $In_{0.20}Ga_{0.80}N/In_{0.05}Ga_{0.95}N$ MQW structure is shown in Fig. 1. The spectrum in sample (a) was composed of three emission bands that are labeled E_{ex1A}, E_D, and E_{lc}, respectively.[14] The E_{lc} band consists of the main peak at

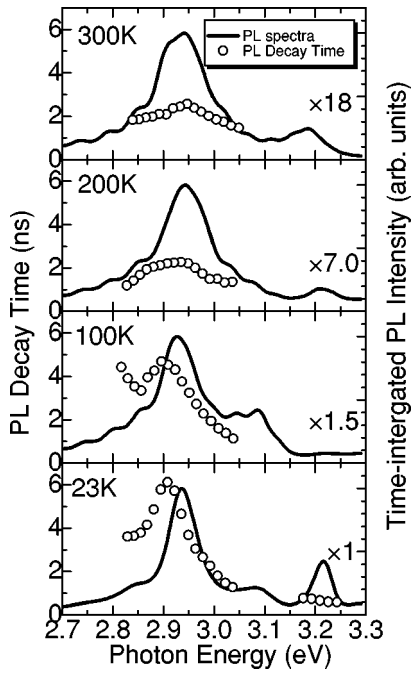

FIG. 2. Time-integrated PL spectra and the PL decay times as a function of monitored emission energy taken at 23, 100, 200, and 300 K, respectively. Excitation energy density was kept constant at 120 nJ/cm^2 in sample (a) ($In_{0.20}Ga_{0.80}N/In_{0.05}Ga_{0.95}N$ MQW).

2.934 eV and LO-phonon sidebands. The TR, ER, and PLE spectroscopy revealed that the transition at 3.216 eV (E_{ex1A}) is due to excitons confined in the lowest quantized level within the well, which is composed of $n=1$ conduction electrons and $n=1$ A (Γ_{9v}) valence holes. The PL transient monitored at the E_D band was well expressed by the double exponential curve whose decay times were 1 and 70 ns. A fast decay component is contributed from the overlapping of neighboring emission bands, while long decay time represents the intrinsic lifetime of this emission band. Since the oscillator strength of this emission is low, this weak E_D band is probably due to the impurity-related centers. An important finding was that the E_{lc} band is attributed to the exciton localized trap center (E_{lc}) within the well. Decay times as well as the rise times of PL are also shown in Fig. 1 as a function of monitored emission energies. The rise time is defined as the time to reach maximum PL intensity after pulsed excitation. At 23 K, decay times monitored in the vicinity of the E_{ex1A} band are almost constant at 600 ps, which is much smaller than those at the E_{lc} band. The rise times of the E_{ex1A} band were constant at about 100 ps, while the rise times of the E_{lc} band changed with photon energy in the range from 200 ps to 900 ps whose dependence was almost the same as that of PL decay times. These features indicate that photogenerated excitons are transferred from the $n=1$ quantized level (E_{ex1A}) to the localized centers.

The time-integrated PL spectra and PL decay times as a function of emission energies at 23, 100, 200, and 300 K in sample (a) are shown in Fig. 2. Decay times in the main PL band (E_{lc}) increase with decreasing monitored photon energies down to about 2.90 eV (Ref. 15) at low temperature below about 150 K. In fact, TRPL spectra revealed the redshift of the peak energies with increasing time after the pulsed photoexcitation. The redshift observed at $t=40$ ns

was about 30 meV at 23 K. These phenomena can be explained by a few models as discussed below.

(i) There exists a large piezoelectric field, which is induced by the biaxial stress in the $In_xGa_{1-x}N$ layer, across the (0001)-oriented strained QW's.[17] Such an internal electric field causes the quantum confined Stark effect (QCSE), where the transition energies as well as the oscillator strength of excitons are lowered compared to the zero-field condition. Just after the excitation, a large number of excitons screen the electric field. However, the screening effect is lowered as the radiative recombination proceeds. Therefore, the redshift with time may be understood as the temporal behavior of QCSE. Such phenomena are observed in the $GaN/Al_xGa_{1-x}N$ QW's with thicker well layer thickness.[16] According to the literature,[17] the induced piezoelectric field and the resulting Stark shift of sample (a) are estimated to be about 1×10^6 V/cm and a few tens meV, respectively.

(ii) If the In compositions within the QW layer are randomly fluctuated, excitons generated by photoexcitation are localized to local potential minima and recombine radiatively. Such a localization process causes a large band-filling effect and may account for the TRPL data.[18] If the density of the tail states is approximated as $\exp(-E/E_0)$ (E_0 represents the degree of the depth in the tail state), and if the radiative lifetime (τ_{rad}) does not change with emission energy, it is possible to estimate the E_0 and the τ_{rad} values by fitting the experimental decay data [$\tau(E)$] with the theoretical equation.[19] In fact, we obtained these values in our structure as $E_0=33.3$ meV and $\tau_{rad}=5.34$ ns at 20 K under $I_{ex}=210$ nJ/cm^2, assuming this model.[6] The universal behavior has been reported in this weak-localization model, where the ratio between the Stokes shift and the exciton absorption linewidth is about 0.6, which is independent on the system.[20]

(iii) If model (ii) is the case, the linewidth of E_{lc} is estimated to be about 400 meV using the Stokes shift corresponding to the energy difference between E_{ex1A} and E_{lc} (250 meV). However, the PL linewidth is about 80 meV which is much smaller than the expected value. Moreover, the Stokes shift is much larger than the peak shift observed in the TRPL measurement. Therefore, it is reasonable to presume that the QD-like region rather than the small fluctuation of In composition is self-formed within the QW due to the compositional modulation. In fact, isotropic QD structures, which are composed of In-rich $In_xGa_{1-x}N$ alloys with the average diameter of about 3 nm, were observed in sample (a) by the structural analysis.[8] In this case, almost isotropic confinement to the QD's lowers the effect of a piezoelectric field compared to the case of uniform QW, and the broadness of the PL spectrum is due to the size and/or compositional fluctuation of QD's, as well as due to the component of higher quantized levels within QD's. Therefore, macroscopic optical data do not reflect the property of singular QD, but should be interpreted as the ensemble of many QD's whose energy levels are distributed inhomogeneously. The transient PL in this case may be attributed to the transfer process from upper quantized levels towards the lowest level and also to the size and/or compositional dependence on the radiative lifetime (τ_{rad}). The difference between models (ii) and (iii) should also be noted. In the case of model (ii), excitons are mobile within the local potential mimima under elevated temperature or high injection levels, and energy levels of localized states are interconnected with the extended states. However, in the case of model (iii), the transfer probability between localized centers is very low, and such centers are energetically separated from extended states.

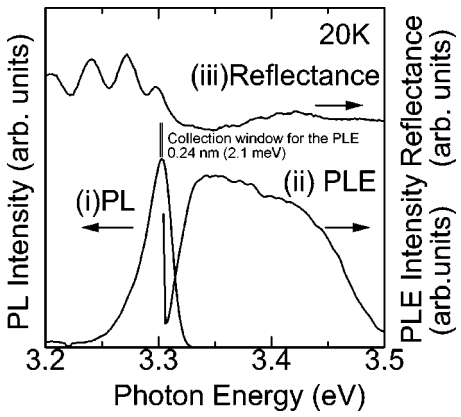

FIG. 3. (i) PL spectrum taken at sample (b). (ii) PLE spectrum. The collection window for the detection is shown in the figure. (iii) Reflectance spectrum. Whole spectra are taken at 20 K.

As shown in Fig. 2, the dependence of the emission energy on the PL decay times became less dominant with increasing temperature. Since the piezoelectric field is expected to be almost constant with temperature, the piezoelectric effect may not play an important role in this particular sample. If the In-rich active region (QD) is surrounded by the In-poor region isotropically, QD is almost under hydrostatic stress as a result of the reduction of the biaxial term. This may be the reason why the effect of the piezoelectric field is not significant in this sample. Therefore, model (iii) is the most feasible one for sample (a) at the current stage. Nevertheless, the maximum decay time observed at around the peak of the E_{lc} band almost represents the τ_{rad} value of the localized excitons. The radiative recombination lifetime (τ_{rad}) of localized excitons (E_{lc}) was estimated to be 6.3 ns at 23 K, assuming the nonradiative recombination lifetime (τ_{nonrad}) is much larger than the τ_{rad} at this temperature. This value is more than one order of magnitude larger than the reported τ_{rad} values of free exciton in GaN single epilayers.[21–23] This is probably a result of the mesoscopic effect, where the oscillator strength of excitons is reduced with decreasing the radius of quantum dots if the wave-vector selection rule is taken into account between the radiation field and the exciton center-of-mass motion.[24]

Figure 3 shows the PL spectrum at 20 K taken at sample (b) whose active layer is composed of the Si-doped $In_{0.10}Ga_{0.90}N$ (3 nm)/$In_{0.02}Ga_{0.98}N$ (6 nm) MQW with three periods. The PL spectrum from the active layer consists of a single peak located at 3.303 eV with the linewidth of 28 meV. It was difficult for this particular sample to apply proper electric field to the *pn* junction at this cryogenic temperature because of the freezing out of carriers. Therefore, PLE and reflectance measurements were performed instead of PV or ER spectroscopy as depicted in Fig. 3 [(ii) and (iii)], although it is difficult to observe a clear absorption edge in the reflectance spectrum due to interference fringes. Both absorption spectra (reflectance and PLE) suggest that the Stokes shift is approximately a few tens meV at 20 K. This value is one order of magnitude smaller than that of

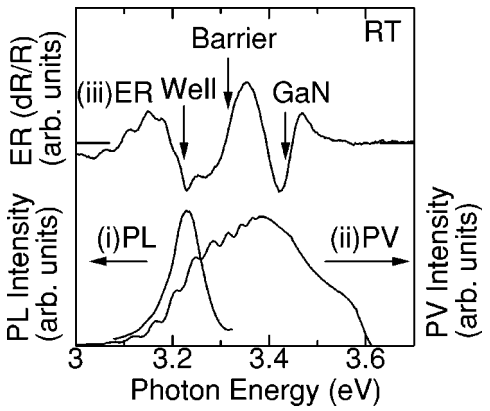

FIG. 4. (i) PL spectrum taken at sample (b). (ii) PV spectrum. (iii) ER(dR/R) spectrum. Whole spectra are taken at 300 K (RT).

sample (a). Figure 4 shows the PL, PV, and ER spectra at RT obtained in sample (b). The absorption edges of the $In_{0.10}Ga_{0.90}N$ well layer, $In_{0.02}Ga_{0.98}N$ barrier layer, and GaN cladding layer were roughly located at 3.23 eV, 3.32 V, and 3.43 eV, respectively. Therefore, almost no Stokes shift is observed in the main PL peak.[25] Since the degree of localization is so small for this sample, the excitons involved in the radiative recombination become free (two-dimensional) at RT due to the thermalization. Such a weak localization at low temperature is probably attributed to model (ii), which probably originates from small potential fluctuation of either In composition or well width.

Figure 5 shows PL decay times of sample (b) at 20 K as a function of monitored emission energies. Time-integrated PL is also inserted in the figure. Decay times increase with decreasing emission energies and tend to saturate on the low-energy side of the band. This can be understood as the effect of exciton localization, where decay of excitons is not only due to radiative recombination but also due to transfer process to the low-energy tail. Theoretical analysis[6] of the PL decay time as a function of emission energy was done assuming the density of tail state as the form of $\exp(-E/E_0)$. The best fitting was obtained using values as $\tau_{rad}=460$ ps and $E_0=15$ meV as shown by the dotted curve in Fig. 5. This E_0 value (degree of localization) fairly accounts for the

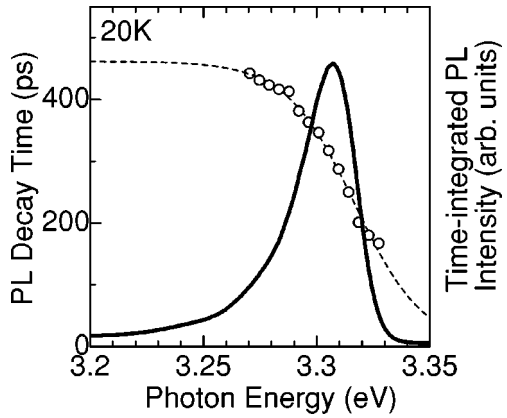

FIG. 5. Time-integrated PL spectrum as well as PL decay times as a function of monitored emission energy taken at 20 K under excitation energy density of 500 nJ/cm^2 in sample (a) ($In_{0.10}Ga_{0.90}N/In_{0.02}Ga_{0.98}N$ MQW).

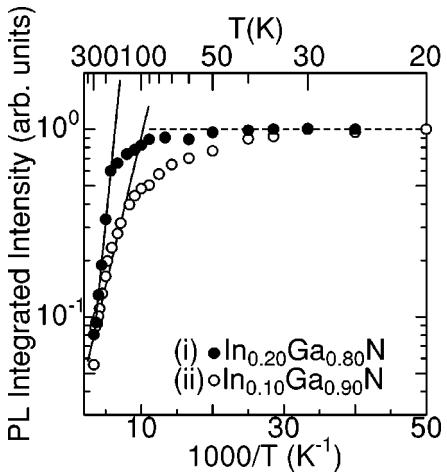

FIG. 6. Integrated PL intensity of (i) E_{lc} band in sample (a) ($In_{0.20}Ga_{0.80}N/In_{0.05}Ga_{0.95}N$ MQW) and (ii) the main band in sample (b) ($In_{0.10}Ga_{0.90}N/In_{0.02}Ga_{0.98}N$ MQW) plotted as a function of $1000/T$. The scale of T is also shown at the upper axis. The quantum efficiency (η) of this emission band is estimated to be 8% for sample (a) and 5% for sample (b) at RT if the η value at the lowest temperature is assumed to be unity.

result where the exciton is almost delocalized at RT due to the thermal energy.

Radiative and nonradiative processes change with temperature (T). The PL decay time measured as a function of temperature [$\tau_{PL}(T)$] is expressed by the following equation:

$$\frac{1}{\tau_{PL}(T)}=\frac{1}{\tau_{rad}(T)}+\frac{1}{\tau_{nonrad}(T)}, \tag{1}$$

where $\tau_{rad}(T)$, $\tau_{nonrad}(T)$ are radiative lifetime and nonradiative lifetime at T K, respectively.

The internal quantum efficiency [$\eta(T)$] can also be written in terms of $\tau_{rad}(T)$ and $\tau_{nonrad}(T)$, where

$$\eta(T)=\frac{\tau_{nonrad}(T)}{\tau_{rad}(T)+\tau_{nonrad}(T)}. \tag{2}$$

Therefore, it is possible to estimate the temperature dependence of radiative and nonradiative lifetimes by monitoring both $\tau_{PL}(T)$ and $\eta(T)$.[26]

Figure 6 shows temperature dependence of the integrated PL intensity [$I(T)$] of the main PL band in (i) sample (a) and (ii) sample (b), in which the $I(T)$ value at the lowest temperature is normalized to unity. The $I(T)$ values in sample (a) were almost constant in the temperature region 23–100 K and then decreased sharply with temperature above about 150 K. While the $I(T)$ values in sample (b) were constant in the lower temperature region 20–40 K and then decreased sharply with temperature above about 100 K. The activation energy (E_A) of PL quenching is estimated to be 75 meV and 31 meV for samples (a) and (b), respectively. The difference of the E_A value reflects that the temperature dependence of the captured cross section to the nonradiative centers varies according to the degree of localization. The internal quantum efficiency at RT of sample (a) (about 8%) is slightly larger than that of sample (b) (about 5%). This may be because the pathway to the nonradiative recombination channel is hin-

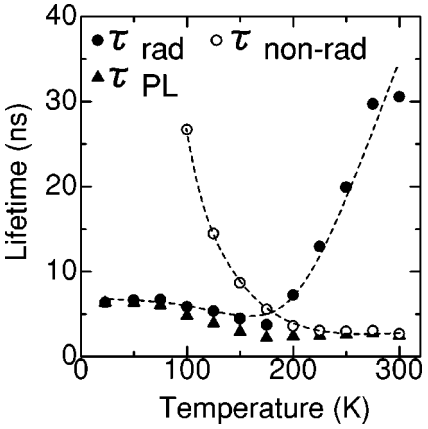

FIG. 7. Temperature dependence of τ_{PL}, τ_{rad}, and τ_{nonrad} values of the localized excitons in sample (a) ($In_{0.20}Ga_{0.80}N/In_{0.05}Ga_{0.95}N$ MQW) that are evaluated by Eqs. (1) and (2).

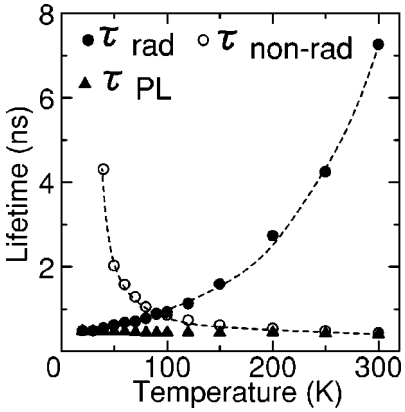

FIG. 8. Temperature dependence of τ_{PL}, τ_{rad}, and τ_{nonrad} values of the localized excitons in sample (b) ($In_{0.10}Ga_{0.90}N/In_{0.02}Ga_{0.98}N$ MQW) that are evaluated by Eqs. (1) and (2).

dered more effectively in sample (a) because excitons are localized to small volume even at RT.

Figures 7 and 8 show temperature dependence of $\tau_{PL}(T)$, $\tau_{rad}(T)$, and $\tau_{nonrad}(T)$ values of localized excitons in (i) sample (a) and (ii) sample (b), respectively. The τ_{rad} values in sample (a) stay almost constant around 6 ns between 23 K and 200 K (Fig. 7). This feature agrees with the theoretical prediction, where the radiative recombination lifetime does not change with temperature for the exciton confined in the quasi-zero-dimensional (0D) potential because the thermalization of excitons in the k (momentum) space is prohibited due to the 0D DOS, which is expressed by the delta function.[24,27] However, $\tau_{rad}(T)$ values in sample (a) increased above 200 K and reached about 30 ns at 300 K (RT). This may be because the excitons confined in the lowest quantized levels within the QD-like region are thermalized to higher subbands. Moreover, it is necessary to take into account the fact that these analyses based on Eqs. (1) and (2) are valid if excitons selectively photogenerated in the wells are not captured by the nonradiative centers before trapped by the quantum dots. If the assumption mentioned above collapses, the number of excitons confined in the QD's reduces as temperature increases, and then radiative lifetimes are overestimated. This effect can be evaluated by the TRPL spectroscopy under the condition where the photoexcitation is tuned selectively to the higher band of QD centers. Our recent result shows that the $I(300\ \mathrm{K})$ is estimated to be about 10% if the QD centers are selectively excited. Therefore, the $\tau_{rad}(300\ \mathrm{K})$ value must probably be modified by a factor of 0.8. Nevertheless, the τ_{rad} value at RT is at most about five times as large as that at 23 K in sample (a).

On the other hand, the τ_{rad} values in sample (b) were constant at 460 ps between 20 K and 40 K, and then increased linearly with the slope of 10 $\mathrm{ps\,K^{-1}}$ from 40 K to 150 K (Fig. 8). Such a T-linear dependence of τ_{rad} values represents the two-dimensional (2D) feature of excitons.[12] It is considered that excitons are localized at the potential minima in the QW at low temperature, and then are delocalized by thermal energy with increasing temperature. As a result, the dimensionality of excitons in sample (b) exhibits nearly 2D character at RT.

IV. CONCLUSION

Dynamical behavior of excitons based on localization, radiative, and nonradiative processes has been studied in (a) $In_{0.20}Ga_{0.80}N/In_{0.05}Ga_{0.95}N$ and (b) $In_{0.20}Ga_{0.80}N/In_{0.05}Ga_{0.95}$ MQW LD structures by means of TRPL spectroscopy. It was found that the dimensionality of excitons is a 0D character for the In-rich QW's [sample (a)], while a 2D character for the In-poor QW's [sample (b)].

ACKNOWLEDGMENTS

The authors are grateful to K. Sawada, K. Omae, and S. Saijou for their assistance in the TRPL measurement. A part of this measurement was done using the facility at the Venture Business Laboratory (VBL) in Kyoto University.

[1] S. Nakamura, M. Senoh, S. Nagahama, N. Iwasa, T. Yamada, T. Matsushita, Y. Sugimoto, and H. Kiyoku, Appl. Phys. Lett. **69**, 4056 (1996).

[2] S. Nakamura, M. Senoh, S. Nagahama, N. Iwasa, T. Yamada, T. Matsushita, Y. Sugimoto, and H. Kiyoku, Appl. Phys. Lett. **70**, 1417 (1997).

[3] S. Nakamura, M. Senoh, S. Nagahama, N. Iwasa, T. Yamada, T. Matsushita, H. Kiyoku, Y. Sugimoto, T. Kozaki, H. Umemoto, M. Sano, and K. Chocho, Appl. Phys. Lett. **72**, 2014 (1998).

[4] S. Nakamura, M. Senoh, S. Nagahama, N. Iwasa, T. Yamada, T. Matsushita, H. Kiyoku, Y. Sugimoto, T. Kozaki, H. Umemoto, M. Sano, and K. Chocho, Jpn. J. Appl. Phys., Part 2 **36**, L1568 (1997).

[5] S. Chichibu, T. Azuhata, T. Sota, and S. Nakamura, Appl. Phys. Lett. **69**, 4188 (1997).

[6] Y. Narukawa, Y. Kawakami, Sz. Fujita, Sg. Fujita, and S. Nakamura, Phys. Rev. B **55**, R1938 (1997).

[7] A. Satake, Y. Masumoto, T. Miyajima, T. Asatsuma, F. Nakamura, and M. Ikeda, Phys. Rev. B **57**, R2041 (1998).

[8] Y. Narukawa, Y. Kawakami, M. Funato, Sz. Fujita, Sg. Fujita,

and S. Nakamura, Appl. Phys. Lett. **70**, 868 (1997).
[9] C. Kisielowski, Z. Liliental-Weber, and S. Nakamura, Jpn. J. Appl. Phys., Part 1 **36**, 6932 (1997).
[10] S. Chichibu, K. Wada, and S. Nakamura, Appl. Phys. Lett. **71**, 2346 (1997).
[11] H. Gotoh, H. Ando, T. Takagahara, H. Kamada, A. Chavez-Pirson, and J. Temmyo, Jpn. J. Appl. Phys., Part 1 **36**, 4204 (1997).
[12] P. Lefebvre, J. Allégre, B. Gil, A. Kavokine, H. Mathieu, W. Kim, A. Salvador, A. Botchkarev, and H. Morkoç, Phys. Rev. B **57**, R9447 (1998).
[13] S. Nakamura, Jpn. J. Appl. Phys., Part 2 **30**, L1705 (1991).
[14] The transition energies at 23 K are slightly different from those of a previous paper (Ref. 6) because of the distribution of transition energies within the epilayer.
[15] Decay times then decrease below about 2.90 eV. This is probably because of the decay component arising from the high-energy side of the 1 LO-phonon replicated band.
[16] J. S. Im, H. Kollmer, J. Off, A. Sohmer, F. Scholz, and A. Hangleiter, Phys. Rev. B **57**, R9435 (1998).
[17] T. Takeuchi, S. Sota, M. Katsuragawa, M. Komori, H. Takeuchi, H. Amano, and I. Akasaki, Jpn. J. Appl. Phys., Part 2 **36**, L382 (1997).
[18] P. G. Eliseev, P. Perlin, J. Lee, and M. Osinski, Appl. Phys. Lett. **71**, 569 (1997).
[19] C. Gourdon and P. Lavallard, Phys. Status Solidi B **153**, 641 (1989).
[20] F. Yang, M. Wilkinson, E. J. Austin, and K. P. O'Donnell, Phys. Rev. Lett. **70**, 323 (1993).
[21] C. I. Harris, B. Monemar, H. Amano, and I. Akasaki, Appl. Phys. Lett. **67**, 840 (1995).
[22] W. Shan, X. C. Xie, J. J. Song, and B. Goldenberg, Appl. Phys. Lett. **67**, 2512 (1995).
[23] Y. Kawakami, Z. P. Peng, Y. Narukawa, Sz. Fujita, Sg. Fujita, and S. Nakamura, Appl. Phys. Lett. **69**, 1414 (1996).
[24] M. Sugawara, Phys. Rev. B **51**, 10 743 (1995).
[25] Preliminary calculation shows that the piezoelectric field (about 0.6 MV/cm) is almost compensated by the built-in potential between the *pn* junction whose direction of the field is opposite to that of the piezo effect.
[26] R. C. Miller, D. A. Kleinman, W. A. Nordland, Jr., and A. C. Gossard, Phys. Rev. B **22**, 863 (1980).
[27] J. Feldmann, G. Peter, E. O. Göbel, P. Dawson, K. Moore, C. Foxon, and R. J. Elliot, Phys. Rev. Lett. **20**, 2337 (1987).